

1-12313



Energy, Mines and  
Resources Canada

Energie, Mines et  
Ressources Canada

**CANMET**

Canada Centre  
for Mineral  
and Energy  
Technology

Centre canadien  
de la technologie  
des minéraux  
et de l'énergie

RADON-222,  $^{220}\text{Rn}$ , AND PROGENY CONCENTRATION LEVELS IN UNDERGROUND  
U/Th ENVIRONMENTS

J. BIGU

ELLIOT LAKE LABORATORY

DECEMBER 1989

MRL 90-49(J)

To be submitted for publication in Journal of Radioanalytical and Nuclear  
Chemistry.

CROWN COPYRIGHT RESERVED

MINING RESEARCH LABORATORY  
DIVISION REPORT MRL 90-49(J)

RADON-222,  $^{220}\text{Rn}$ , AND PROGENY CONCENTRATION LEVELS IN UNDERGROUND  
U-Th ENVIRONMENTS

J. Bigu\*

ABSTRACT

Airborne concentration levels of  $^{222}\text{Rn}$  and its progeny, and  $^{220}\text{Rn}$  progeny were measured in an underground U mine. In addition, concurrent measurements of several meteorological variables such as temperature, relative humidity, barometric pressure and airflow rate were also carried out. Mining operations and mining activities during the measurements were carefully noted. The data collected show great variability. Although not particularly strong, some definite correlations could be found between airborne radioactivity concentration levels, meteorological variables, and mining operations (and mining activities). The difficulty in obtaining stronger correlations between the above variables is attributed to the great and simultaneous variability of most of the variables measured. The data presented here are typical of 'active' U-Th mining environments, i.e., of Ontario (Canada) underground U mines. Measurements extended for a period of a full calendar year and involved several thousand independent measurements.

---

Key words: Radon and its progeny; Thoron and its progeny; Uranium; Thorium; Uranium mines.

\*Research Scientist Elliot Lake Laboratory, CANMET, Energy, Mines and Resources Canada, Elliot Lake, Ontario, Canada, P5A 2J6.

## INTRODUCTION

Uranium and Th minerals are widely distributed in the crust of the earth. These two radioelements, i.e.,  $^{238}\text{U}$  and  $^{232}\text{Th}$ , are the parents of two naturally occurring radioactive decay chains. (Although  $^{235}\text{U}$  is the parent of another radioactive decay chain, its occurrence in nature is very low compared to that of  $^{238}\text{U}$ , and hence, is not considered here.) Through a series of radioactive decays,  $^{238}\text{U}$  and  $^{232}\text{Th}$  form two radioactive gases,  $^{222}\text{Rn}$  and  $^{220}\text{Rn}$ , respectively. Because of their gaseous nature,  $^{222}\text{Rn}$  and  $^{220}\text{Rn}$  readily diffuse through rock formations, and structural and building materials, finding their way into working and living spaces, where they further decay into their respective progeny.

The airborne concentrations of  $^{222}\text{Rn}$ ,  $^{220}\text{Rn}$ , and their progeny, in a given enclosure such as a mine, cavern, building, or any other partially or totally enclosed environment tell us a great deal about the geometry and ventilation of these environments, as well as of the physico-chemical properties of, and U and Th concentrations in, the materials making up these enclosures. It is generally recognized that ratios of some radioactivity variables are of sufficient practical interest from the ventilation, engineering, occupational and health physics standpoints to justify their measurement.

The radioactivity and meteorological data reported here were collected in a hard rock underground (UG) U mine, located in the Elliot Lake (ON, Canada) area and at a depth of 500-700 m. The ore grade (U) was ~0.2-0.3%. For this region the ratio Th/U is in the approximate range <1 to ~4.

## EXPERIMENTAL CONSIDERATIONS AND PROCEDURES

Underground measurements were divided into four categories, namely, radioactivity measurements, meteorological measurements, physical and geometrical measurements, and observations of the physical appearance of locations of the mine where measurements were taken.

The following radioactivity and meteorological variables were measured:  $^{222}\text{Rn}$  and  $^{220}\text{Rn}$  concentrations,  $^{222}\text{Rn}$  and  $^{220}\text{Rn}$  progeny concentrations, temperature (T), relative humidity (RH), airflow rate (Q), air residence times (RT), and barometric pressure (P).

Measurements were made by conventional grab-sampling techniques. Radon-222 and  $^{220}\text{Rn}$  progeny concentrations were measured using the Kusnetz<sup>1</sup> and Rock<sup>2</sup> methods, respectively. The

values for these two variables are given here as the Potential Alpha Energy Concentration (PAEC, in  $\mu\text{Jm}^{-3}$ ) and in the more conventional and historical Working Level units, WL(Rn) and WL(Tn). Radon-222 concentration was measured using scintillation cell techniques, whereas  $^{220}\text{Rn}$  concentration measurements were conducted using the Two Filter Tube (2FT) method<sup>3</sup>.

Airflow rate and residence times were estimated by conventional anemometry measurements. Temperature, relative humidity and barometric pressure were carefully noted in a multitude of mine locations. Data were taken for a large number of mine locations in the presence and absence of several mining operations, and other mining activities, such as vehicle traffic and the like.

The radioactivity and meteorological survey conducted at this UG U mine lasted one complete calendar year and consisted of several thousand independent measurements.

## EXPERIMENTAL RESULTS AND DISCUSSION

A summary of the data obtained is given in Figs. 1-10 and Tables 1 and 2. The graphical data are given in the form of normalized frequency histograms for each of the variables considered. The data shown in these histograms are not specific to a particular area of the mine, but rather they are representative of the entire UG mine environment.

Figure 1 shows the  $^{222}\text{Rn}$  concentration frequency histogram. The figure indicates that  $>80\%$  of the measurements fall within the range  $370 \text{ Bqm}^{-3}$  ( $10 \text{ pCiL}^{-1}$ ) to  $1,295 \text{ Bqm}^{-3}$  ( $35 \text{ pCiL}^{-1}$ ). The figure also shows two distinct distributions, namely, a low concentration distribution centered at about  $740 \text{ Bqm}^{-3}$  ( $20 \text{ pCiL}^{-1}$ ) and a high concentration distribution centered at approximately  $3.14 \times 10^3 \text{ Bqm}^{-3}$  ( $85 \text{ pCiL}^{-1}$ ).

Figure 2 shows the  $^{222}\text{Rn}$  progeny concentration level [PAEC(Rn) and WL(Rn)] histogram. The values for these variables ranged from  $<1.04 \mu\text{Jm}^{-3}$  [ $<0.05 \text{ WL(Rn)}$ ] to  $\sim 30 \mu\text{Jm}^{-3}$  [ $\sim 1.4 \text{ WL(Rn)}$ ]. However, apart from a few ( $\sim 6\%$ ) relatively high values ( $\sim 26\text{-}30 \mu\text{Jm}^{-3}$ ) measured, the distribution of values found for the  $^{222}\text{Rn}$  progeny was mainly concentrated in two concentration regions centered at about  $1.04\text{-}2.08 \mu\text{Jm}^{-3}$  and  $9.4\text{-}10.4 \mu\text{Jm}^{-3}$ .

Figures 1 and 2 show a similar pattern: two well separated frequency distributions in each case, centered at two relatively well defined values. From these data, one may conclude that there is a definite correspondence between  $^{222}\text{Rn}$  progeny concentrations, e.g., PAEC(Rn), and [ $^{222}\text{Rn}$ ]. It is also worth noting that although the [ $^{222}\text{Rn}$ ] distributions are reasonably symmetrical,

their PAEC(Rn) counterparts are skewed. The reason for this is that the  $^{222}\text{Rn}$  progeny are strongly affected by mine aerosol concentration and particle size distribution, variables which have no effect on  $[\text{}^{222}\text{Rn}]$ .

Aerosol concentration and particle size distribution affect the plate-out of  $^{222}\text{Rn}$  progeny on large surfaces such as mine walls. A variety of aerosols within a wide particle size range are produced in mine environments in the course of mining operations, vehicle traffic, and other mining activities, particularly in heavily 'dieselized' mines such as the one under study. However, aerosol concentration and particle size distribution can vary largely depending on mining operations and other mining activities, or the lack thereof. Particle concentration in mine environments can easily range from  $\sim 1.0 \times 10^3 \text{ cm}^{-3}$  for 'inactive' areas to  $>10^5 \text{ cm}^{-3}$  for mining operations using diesel equipment. Furthermore, the particle size can range from submicron size aerosols ( $\sim 0.05 \mu\text{m}$  to  $<1 \mu\text{m}$ ) to dust in the 'respirable' range ( $\sim 1 \mu\text{m}$  to  $\sim 10 \mu\text{m}$ ).

From the above discussion, one may surmise that although the correspondence between  $^{222}\text{Rn}$  progeny concentration, e.g., PAEC(Rn), and  $[\text{}^{222}\text{Rn}]$  should be expected and is a rather trivial consequence of these radioactivity environments, the reader should be cautioned that this is far from true since it is easy to verify experimentally that it is possible, and quite frequent, to have in two distinct locations:

1. The same  $[\text{}^{222}\text{Rn}]$  with quite different  $^{222}\text{Rn}$  progeny concentrations and disequilibrium ratios, or
2. Quite different  $[\text{}^{222}\text{Rn}]$  with similar  $^{222}\text{Rn}$  progeny concentrations.

Items 1 and 2 are, however, easily predictable on theoretical grounds if plate-out phenomena considerations are taken into account. As would be anticipated, both  $[\text{}^{222}\text{Rn}]$  and  $^{222}\text{Rn}$  progeny are related to (dependent on) airflow conditions in the mine. This is discussed below in conjunction with Figs 1, 2, 3, and 7.

Figure 3 shows the frequency histogram corresponding to the disequilibrium factor, or F-factor, defined as the ratio of  $^{222}\text{Rn}$  progeny concentration to the corresponding  $^{222}\text{Rn}$  concentration. In the 'historical' units of Working Level (WL) and  $\text{pCiL}^{-1}$ ,  $F = \text{WL(Rn)} \times 10^2 / [\text{}^{222}\text{Rn}]$ . Preferred definitions are, however,  $F = \text{PAEC} / \text{PAEC}^*$ , where  $\text{PAEC}^*$  is the PAEC that would exist with all short-lived  $^{222}\text{Rn}$  progeny in equilibrium with  $^{222}\text{Rn}$ . Alternatively,  $F = \text{EEC} / [\text{}^{222}\text{Rn}]$ , where EEC is the equilibrium equivalent  $^{222}\text{Rn}$  concentration. The three definitions for F give the same result, namely,  $0 \leq F \leq 1$ . Figure 3 shows a wide range of values for F, namely, from 0.1 to 1.2, with most of the measurements between 0.1 and 0.6. However,

a closer look at Fig. 3 suggests a 'multimodal' distribution the maxima centered at 0.2, 0.5, 0.8, and 1.2, but with most of the F-values (~94%) centered at 0.2 and 0.5. (Multivalued distributions seem to apply also to [ $^{222}\text{Rn}$ ] and  $^{222}\text{Rn}$  progeny concentrations when Figs. 1 and 2 are inspected in more detail.)

The broad distribution of values shown in Fig. 3 suggests that attempts at calculating PAEC, and hence WL(Rn), from, say, passive measurements of  $^{222}\text{Rn}$  activity concentration levels by charcoal canisters, track etch detectors, and other devices, are not reliable and are subject to great uncertainty. Most of the manufacturers, distributors, mine operators, and in general, users of these devices assume  $F = 0.3$  (in 'old units') to calculate  $^{222}\text{Rn}$  progeny concentration from  $^{222}\text{Rn}$  measurements.

The above figure also shows some values ( $\leq 1\%$ ) for which  $F > 1$ . Although, in principle not theoretically possible, values for the disequilibrium factor greater than unity have been observed by the author on a number of occasions in UG U mines, even in cases for which the concentration levels of  $^{222}\text{Rn}$  and its progeny were high enough for accurate measurement, thereby eliminating the problem of poor counting statistics, and the like<sup>4</sup>. However, in environments in which aerosols, do not behave like an ideal gas (any real environment) it is possible in the view of some researchers, to have values of  $F$  greater than unity.

Figure 4 shows the frequency histogram of the  $^{220}\text{Rn}$  concentration, [ $^{220}\text{Rn}$ ]. The values shown were obtained by a semi-empirical approach discussed elsewhere<sup>5</sup>. The histogram shows a wide range of values from very low values to about  $3.3 \times 10^3 \text{ Bqm}^{-3}$  ( $90 \text{ pCiL}^{-1}$ ). Values significantly higher than those indicated in Fig. 4 (not included in the graph) were measured in some selected areas of the mine. Figure 4 can be roughly divided into two defined regions, one with concentration values from close to 0 to  $\sim 250 \text{ Bqm}^{-3}$  and the other with values in the range  $\sim 250$  to  $> 3 \times 10^3 \text{ Bqm}^{-3}$ .

Figure 5 shows the frequency histogram of the  $^{220}\text{Rn}$  progeny concentration level, PAEC(Tn), or WL(Tn). About 80% of the total number of measurements were at or below  $5.2 \mu\text{Jm}^{-3}$  [ $0.25 \text{ WL(Tn)}$ ]. The graph also shows that the  $^{220}\text{Rn}$  progeny concentrations were distributed in two different regions with maxima at  $\sim 2 \mu\text{Jm}^{-3}$  ( $\sim 84\%$ ) and  $\sim 8 \mu\text{Jm}^{-3}$  (16%). Comparison between Figs. 2 and 5 strongly suggest a relationship between PAEC(Rn) and PAEC(Tn). Indeed this is the case as indicated by eqns. 1 and 2, discussed below. This relationship between  $^{222}\text{Rn}$  progeny and  $^{220}\text{Rn}$  progeny should not come as a surprise in a UG U-mine with significant Th concentrations in the rock formation. Finally, a definite, albeit

somewhat weak, relationship between  $[^{220}\text{Rn}]$  and PAEC(Tn) can be appreciated when comparing the two ranges of values (regions) for each variable shown in Figs. 4 and 5, respectively.

Figure 6 shows the frequency histogram of the ratio PAEC(Tn):PAEC(Rn). The graph shows a wide range of values (up to ~7.5) which can be divided as a first approximation into a 'low'-value region with values for the above ratio in the range 0-2 (~68%) and a widely scattered high-value region with values in the range 2-7 (~32%). It is possible to subdivide these two regions into four somewhat arbitrary ranges for the purpose of further analysis with regard to airflow rate considerations (see Fig. 7), namely: 0-0.7, 0.7-2.0, 2.2-3.5, and 3.7-7.5. It has been previously indicated<sup>6</sup> that the ratio PAEC(Tn):PAEC(Rn) is a good indicator of airflow (ventilation) conditions in UG U environments. It can be shown that the ratio of  $^{220}\text{Rn}$  progeny to  $^{222}\text{Rn}$  progeny increases with increasing airflow rate, Q, and consequently with decreasing air residence time, RT. Most values in Fig. 6 are about, or greater than, unity, which for a rock formation with an U to Th gram ratio of about unity, indicates that, in general, the mine is well ventilated (see Fig. 7). Values of much less than unity for the progeny ratio indicate locations of poor ventilation or stagnant air.

The accurate measurement of  $^{222}\text{Rn}$  and  $^{220}\text{Rn}$  progeny levels in  $^{222}\text{Rn}$ ,  $^{220}\text{Rn}$  mine atmospheres is a lengthy and time consuming task that severely limits the number of samples that can be taken for personal dosimetry and ventilation engineering purposes. Because of these limitations, it is important to determine whether there is a relationship between  $^{220}\text{Rn}$  progeny and  $^{222}\text{Rn}$  progeny that can be used to derive one variable from the other with reasonable accuracy, in this case  $^{220}\text{Rn}$  progeny concentration levels from  $^{222}\text{Rn}$  progeny concentration levels. Studies of this nature have been conducted by the author in the past<sup>5</sup>. A similar analysis of the data collected in this investigation using least square fitting techniques shows that the relationship between  $^{220}\text{Rn}$  progeny Working Level and  $^{222}\text{Rn}$  progeny Working Level is given by the following expression:

$$\text{WL(Tn)} = 0.61 \text{ WL(Rn)}^{0.605} ; \text{ C.C.} = 0.7 \quad (1)$$

$$\text{WL(Tn)} = 0.878 \text{ WL(Rn)} + 0.052 ; \text{ C.C.} = 0.86 \quad (2)$$

where, the symbol C.C. stands for correlation coefficient. Equations 1 and 2 were originally derived in conventional Working Level terms instead of SI units. Because the above relationships represent many hundreds of measurements taken that were tabulated for analysis purposes, the best fitted analytical expressions, as originally obtained i.e., in terms of WL(Rn) and WL(Tn), are presented. The above expressions can be converted into their corresponding

PAECs by using the relationship  $PAEC(\mu Jm^{-3})/20.8 = WL$ . Equations (1) and (2) become, respectively:

$$PAEC(Tn) = 2.02 [PAEC (Rn)]^{0.605} \quad (3)$$

$$PAEC(TN) = 0.878 PAEC(Rn) + 1.082 \quad (4)$$

Expressions similar to eqns. 1 and 2, but in SI units, can only be obtained now if the entire analytical procedure is repeated by first converting all the WL's data in PAEC, and then applying the statistical treatment indicated above. However, eqns. 1 and 2 can be used as they are in order to calculate in each case of interest the value in PAEC units by first calculating the WL(Tn) corresponding to a given WL(Rn), and then applying the equality:  $1 WL = 20.8 \mu Jm^{-3}$ .

Although the numerical coefficients of eqns. 1 to 4 are somewhat different from the ones derived from previous expressions for other UG environments, the final values for the variable of interest, i.e., WL(Tn) or PAEC(Tn), are not much different. Equations 1 and 2 are useful in personal exposure and in mine ventilation engineering calculations.

Figure 7 shows the frequency histogram of underground airflow rate, Q, conditions. Although a wide range of values was measured, i.e., from  $\sim 15 m^3s^{-1}$  to  $>85 m^3s^{-1}$ , the histogram suggests that, broadly speaking, Q can be divided into a low Q-region ( $5-10 m^3s^{-1}$ ) and a relatively high Q-region ( $70-85 m^3s^{-1}$ ). (A more detailed analysis of the data indicates a multivalued distribution with maxima at about 15, 25, 40, and  $80 m^3s^{-1}$ ).

Forced air ventilation is the most common method used to reduce or control noxious airborne pollutants, including radioactive elements such as  $^{222}Rn$ ,  $^{220}Rn$ , and their descendants. Assuming no recirculation pathways in the ventilation network, areas of high airflow rates are, in general, characterized by low concentration levels of  $^{222}Rn$ ,  $^{220}Rn$ , and their short-lived decay products. The dependence of  $[^{222}Rn]$ , PAEC(Rn),  $[^{220}Rn]$  and PAEC(Tn) on Q is readily obvious when comparing Figs. 1, 2, 4, and 5 with Fig. 7, respectively.

It has been shown<sup>6</sup> that under steady-state conditions the ratios  $PAEC(Rn):[^{222}Rn]$  and  $PAEC(Tn):[^{220}Rn]$  decrease within decreasing values of the residence time (RT) of mine air in the mine volume (V) under consideration ( $RT = V:Q$ ). In other words, these radioactivity ratios decrease within increasing airflow rates, Q. Inspection of Figs. 3 and 7 shows a distribution of values centered in four regions with maxima at about 0.2, 0.5, 0.8, and 1.2 (Fig.3), and 15, 25, 40, and  $80 m^3s^{-1}$  (Fig. 7). Taking into account the inverse relationship between F and Q indicated above, a simple calculation of the product QF shows a reasonable constant value ranging from  $\sim 900 \mu Jm^3$  to  $\sim 1,120 \mu Jm^3$ , within an average value of  $\sim 1,030 \mu Jm^3$ , and a variation of  $<25\%$



between the maximum and minimum values calculated within the Q range 15-80  $\text{m}^3\text{s}^{-1}$ . These results are quite reasonable, particularly when taking into account that because  $[\text{}^{222}\text{Rn}]$  is mainly affected by Q whereas PAEC(Rn) is affected by other factors (e.g., aerosol concentration, N, and aerosol particle size distribution), in addition to Q, the relationship between the ratio PAEC(Rn): $[\text{}^{222}\text{Rn}]$  and Q is somewhat more complex than the relationship between  $[\text{}^{222}\text{Rn}]$  and Q.

Figures 8 to 10 show, respectively, the frequency histograms corresponding to temperature, relative humidity, and barometric pressure. Although relative humidity and temperature are suspected of influencing the plate-out of radioactive decay products on mine walls, and other large surfaces, the complexity of this UG U-mine environment was such that no clear effect or correlation could be found between these environmental variables and the removal of  $^{222}\text{Rn}$  and  $^{220}\text{Rn}$  progeny on mine walls by plate-out mechanisms. Barometric pressure, on the other hand, is known to influence the transport of interstitial  $^{222}\text{Rn}$  in the rock formation to mine openings. Hence, barometric pressure and transport phenomena are inversely related as repeatedly reported in the literature<sup>7</sup>. However, because of the extreme complexity of the UG environment, it was difficult to verify quantitatively  $^{222}\text{Rn}$  transport phenomena as a function of barometric pressure. The effect of the latter is usually small for the case of very low gas permeability and very low porosity materials such as hard rock (granite) mines. The values for the temperature and relative humidity varied, as expected, with the season. Most values, however, were in the range 12-18°C and 50 to >95%, respectively. The histograms for the temperature and relative humidity are presented here to give the reader an idea of the environmental and working conditions in this particular mine. As for other environmental variables, UG barometric pressure closely followed the surface barometric pressure. Values for the former were in the range 105 to 109 kPa.

Table 1 shows data pertaining to  $^{222}\text{Rn}$ , and its progeny, and  $^{220}\text{Rn}$  progeny concentrations, and some ratios of practical interest involving the above variables, obtained for several representative mine locations and days. Also shown in the table are the mining operations and/or mining activity, e.g., vehicle traffic, and preparations observed during the measurements. However, it should be noted that most of these operations and activities were intermittent in nature, and hence, no complete time record of them during the entire working shift is available. Data shown for a given day represent measurements conducted at several sampling stations within a given mine location. The data tabulated exhibit a great variability within each day and from day to day within a given mine location. The variability of the data within each day can

be inferred indirectly from the standard deviation quoted. The day to day variability can easily be seen directly by simple inspection of the table. The data variability is attributed to:

1. Unpredictable variability in UG airflow conditions, e.g., ventilation doors opening and closing to allow vehicles and machinery through;
2. Passage of vehicles, heavy tools, heavy machinery, and trucks which involve a quite noticeable pushing and pulling action of mine air;
3. Mining operations, e.g., slushing, mucking, drilling, and the like as stated above, are intermittent in nature;
4. Causes such as mine water drainage;
5. Intentional rerouting of ventilation air in the ventilation circuitry;
6. Variations in meteorological conditions underground such as temperature, relative humidity, aerosol and dust concentration and size distribution, and barometric pressure.

Because of items 1 to 6, it is not unreasonable to visualize the great difficulty in establishing a clear correlation between airborne radioactivity (e.g.,  $^{222}\text{Rn}$ ,  $^{220}\text{Rn}$ , and their short-lived decay products) concentration levels and any one of the above items in general, or a given meteorological or environmental variable, mining operation, and the like, in particular. This is so because two, more than two, or all of these variables may be varying simultaneously in a not easily predictable fashion. Multivariable correlation analyses were conducted in order to establish a correlation between radioactivity levels and meteorological data. No clear correlation was found in most cases, for the reasons already indicated. However, in a number of cases for which some experimental conditions, such as airflow rate, remained constant throughout a series of radioactive measurements, it was possible to investigate the influence of some mining operations and mining activities on  $^{222}\text{Rn}$ , PAEC(Rn), and PAEC(Tn). Some of these data are shown in Table 2<sup>4</sup>.

Table 2 shows the effect of some mining operations and activities or the lack thereof, on some radioactivity variable, indicated as the percentage of variation, by the symbol D followed by the variable under consideration. The locations indicated in Table 2 are not necessarily the same as the ones indicated in Table 1. In all the cases shown in this table, the airflow conditions, Q, in the mine locations studied remained relatively constant.

## CONCLUSIONS

The results presented in Figs. 1 to 10 and Table 1 show that great variability in radioactivity and meteorological data in the mine investigated should be expected. Constant conditions in UG mine environments are quite rare, thereby making accurate predictions, and assessment and analysis of radioactive concentration levels somewhat difficult to carry out with the desired degree of confidence. In spite of these experimental difficulties, a number of relationships could be established within a certain degree of confidence between several radioactivity variables, UG airflow conditions, and the presence or absence of certain mining operations and activities. The following dependences were observed between:

- a) [ $^{222}\text{Rn}$ ] and PAEC(Rn), and between these two variables and Q;
- b) PAEC(Tn) and Q;
- c) PAEC(Tn) and PAEC(Rn);
- d) [ $^{222}\text{Rn}$ ], PAEC(Rn), PAEC(Tn), and certain mining operations and activities (see Table 2) and;
- e) F and Q.

The data presented here also give a fair indication of underground conditions in this particular mine. However, it should be pointed out that similar surveys in other mines show similar characteristics and variability of the data. Furthermore, it may be surmised from Table 1 and Fig. 3 that attempts to use the F-factor for calculating the PAEC(Rn) from  $^{222}\text{Rn}$  activity concentration values, as some devices are claimed to be capable of doing, will be quite unreliable because of the great variability of this factor depending on UG conditions. The use of this factor will, however, provide an approximate value for the  $^{222}\text{Rn}$  progeny concentration useful for some practical applications. Finally, and although not directly discussed in this paper, the ratio PAEC(Tn):PAEC(Rn) represents a very good indicator of airflow conditions in UG U mines.

## ACKNOWLEDGEMENTS

The data presented here were collected at Denison Mines Ltd. (Elliot Lake, Ontario, Canada) by mine personnel. The author is particularly grateful to J.L. Chakravatti for helpful technical discussions regarding the data, and for kindly agreeing to the publication of these data. The author is also grateful to D. Schryer for making the data available and for facilitating some

underground measurements. Finally, thanks are also extended to C. Seeber for his assistance in reformatting the data and clarifying many important points.

#### REFERENCES

1. H.L. Kusnetz, Am. Ind. Hyg. Assoc. J. 17 (1956) 1.
2. R.L. Rock, MESA Information Report IR-1015 (U.S. D.O.I) (1975).
3. Y.S. Mayya, P.Kotrappa, Ann. Occup. Hyg. 21 (1978) 169.
4. J. Bigu, CANMET, EMR Canada (Ottawa) Division Report MRL 89-36(TR) (1988).
5. J. Bigu, Health Phys. 55 (1988) 525.
6. J. Bigu, Health Phys. 48 (1985) 371.
7. W.E. Clements and M.H. Wilkening, J. Geophys. Res. 79 (1974) 5025.

## LIST OF CAPTIONS

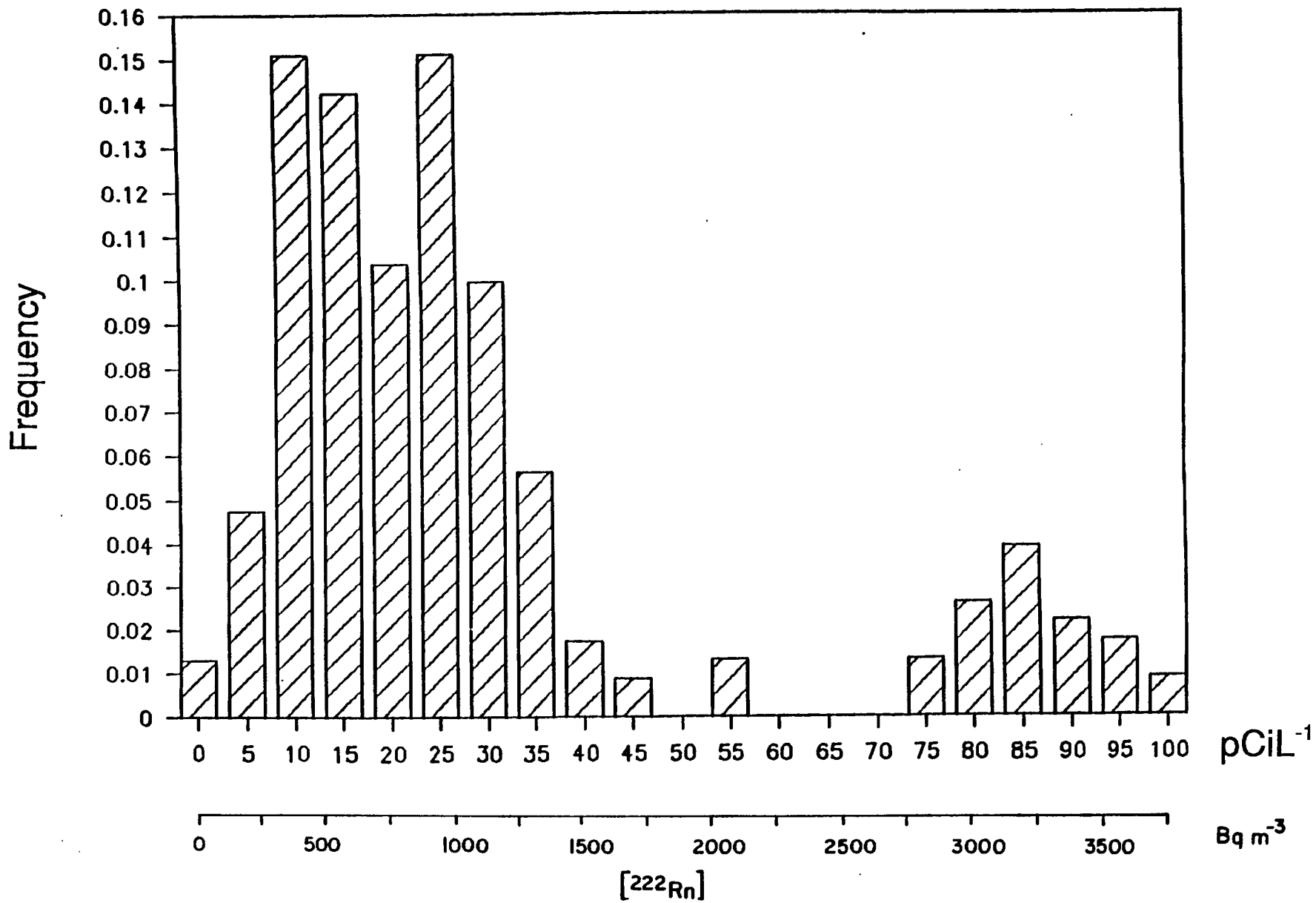
- Fig. 1 - Normalized  $^{222}\text{Rn}$  concentration, [ $^{222}\text{Rn}$ ], histogram.
- Fig. 2 - Normalized  $^{222}\text{Rn}$  progeny concentration histogram: in Potential Alpha Energy Concentration (PAEC), lower scale, and Working Level (WL), upper scale. The symbol Rn is used to indicate  $^{222}\text{Rn}$ .
- Fig. 3 - Normalized F-factor histogram defined as the ratio between  $^{222}\text{Rn}$  progeny concentration and  $^{222}\text{Rn}$  concentration. (The F-factor is given in two types of units, the SI international, lower scale, and 'historical' units, upper scale).
- Fig. 4 - Normalized  $^{220}\text{Rn}$  concentration, [ $^{220}\text{Rn}$ ], histogram.
- Fig. 5 - Normalized  $^{220}\text{Rn}$  progeny concentration histogram: in PAEC, lower scale, and WL, upper scale. The symbol Tn is used to indicate  $^{220}\text{Rn}$ .
- Fig. 6 - Normalized  $^{220}\text{Rn}$  progeny to  $^{222}\text{Rn}$  progeny ratio histogram.
- Fig. 7 - Normalized airflow rate frequency histogram in the mine.
- Fig. 8 - Normalized temperature frequency histogram in the mine.
- Fig. 9 - Normalized relative humidity histogram in the mine.
- Fig. 10 - Normalized barometric pressure histogram in the mine.
- Table 1 - Airborne radioactivity data for several mine operations and days.
- Table 2 - Effect of some mining operations and activities, or lack thereof, on radioactivity levels.

Table 1

Location	Day	$[^{222}\text{Rn}]$ ( $\text{Bqm}^{-3}$ )	PAEC( $\text{Rn}$ ) ( $\mu\text{Jm}^{-3}$ )	PAEC( $\text{Tn}$ ) ( $\mu\text{Jm}^{-3}$ )	F-Factor	$\frac{\text{PAEC}(\text{Tn})}{\text{PAEC}(\text{Rn})}$	Mining Activity
Airway/Travelway	1	335.2±196	0.31±0.21	-	0.16	-	No traffic
	2	101.0±74	0.02±0.06	1.83±0.21	0.22	88.00	" "
	3	180.2±170	0.23±0.21	0.83±0.42	0.22	3.64	" "
	4	89.2±67	0.17±0.08	0.96±0.42	0.33	5.75	" "
	5	373.0±137	0.77±0.21	0.81±0.42	0.37	1.05	" "
Jackleg Stope	1	1,703.0±304	1.83±0.42	2.62±0.42	0.19	1.43	Slushing
	2	1,145.0±170	1.85±0.42	1.46±0.42	0.16	1.40	No traffic, no activity
	3	1,884.0±115	1.77±0.21	1.66±0.21	0.17	0.94	Bolting, scaling
	4	1,601.0±222	1.71±0.08	1.87±0.21	0.19	1.10	No traffic, no activity
	5	2,916.0±684	2.54±0.15	2.08±0.42	0.15	0.87	Bolting, scaling
Area Exhaust	1	343.4±81	0.37±0.15	1.04±2.70	0.19	2.78	Bolting, scaling
	2	194.2±13	0.21	0.62±0.42	0.19	3.00	No traffic, no activity
	3	369.6±164	0.48±0.12	1.10±0.21	0.23	2.30	Diamond drilling
	4	411.4±178	0.62	0.42	0.27	0.67	No traffic, no activity
	5	1,459.0±34	4.58±0.42	2.81±0.21	0.56	0.61	No activity
	6	526.9±0.21	0.52±0.21	1.35±0.21	0.18	2.60	No traffic, no activity
Jumbo Development Heading	1	1,043.0±133	10.19±0.21	2.95±0.62	0.17	2.90	No activity
	2	1,263.0±359	1.81±0.42	2.14±0.23	0.25	1.18	Traffic
	3	1,329.0±494	3.20±2.58	3.43±2.12	0.43	1.07	Traffic
	4	969.0±107	1.04	2.14±0.42	0.19	2.06	Haulage equipment lading
	5	914.0±170	1.41±0.42	-	0.27	-	No traffic, no activity
Mining Area	1	1,259.0±141	2.18±0.31	4.16±1.04	0.31	1.90	No activity
	2	1,383.0±100	4.78	3.74±0.62	0.61	0.78	No traffic, no activity
	3	1,485.0±496	2.91±0.10	3.54±0.83	0.35	1.21	No traffic, no activity
	4	1,114.0±869	3.12±0.23	3.74±0.44	0.50	1.20	No traffic, no activity
	5	1,413.0	2.91	3.33	0.37	1.14	Drilling on face
	6	1,891.0	3.33	3.12	0.31	0.94	Setting up, misc. work

Table 2

Description	Operation	$\Delta[{}^{222}\text{Rn}]$ %	$\Delta[\text{PAEC}(\text{Rn})]$ %	$\Delta[\text{PAEC}(\text{Tn})]$ %
Jackleg stope A	Drilling, slushing	67	149	31
Jackleg stope B	No traffic, drilling	200	0	136
Jackleg stope C	No traffic, setting up	21	12	?
Travelway A	No traffic, setting up	53	0	90
Travelway B	No traffic, traffic	83	33	-19
Exhaust airway	No traffic, traffic	32	21	104
Crusher decline	No traffic, traffic	19	0	-21



ig. 1



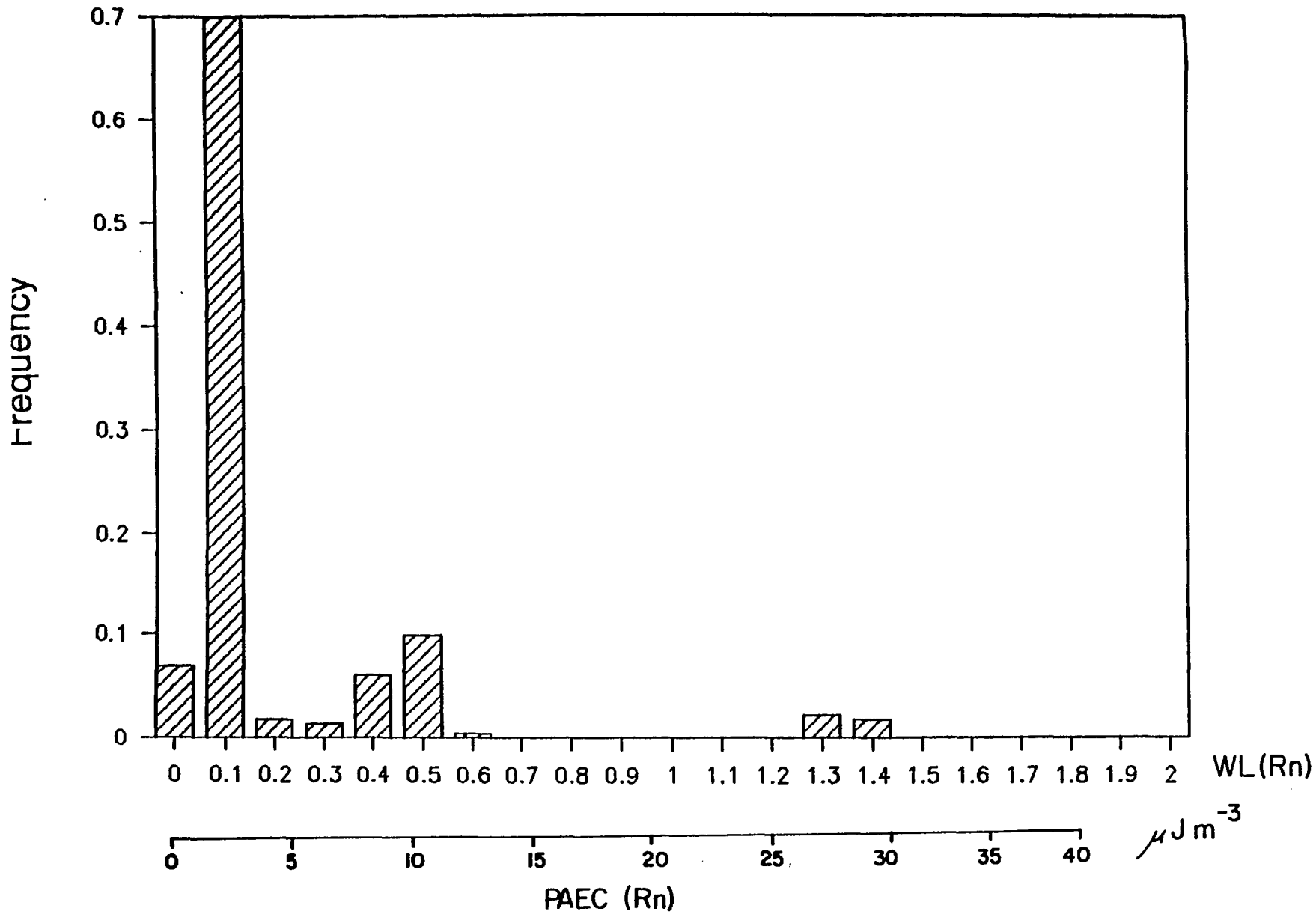
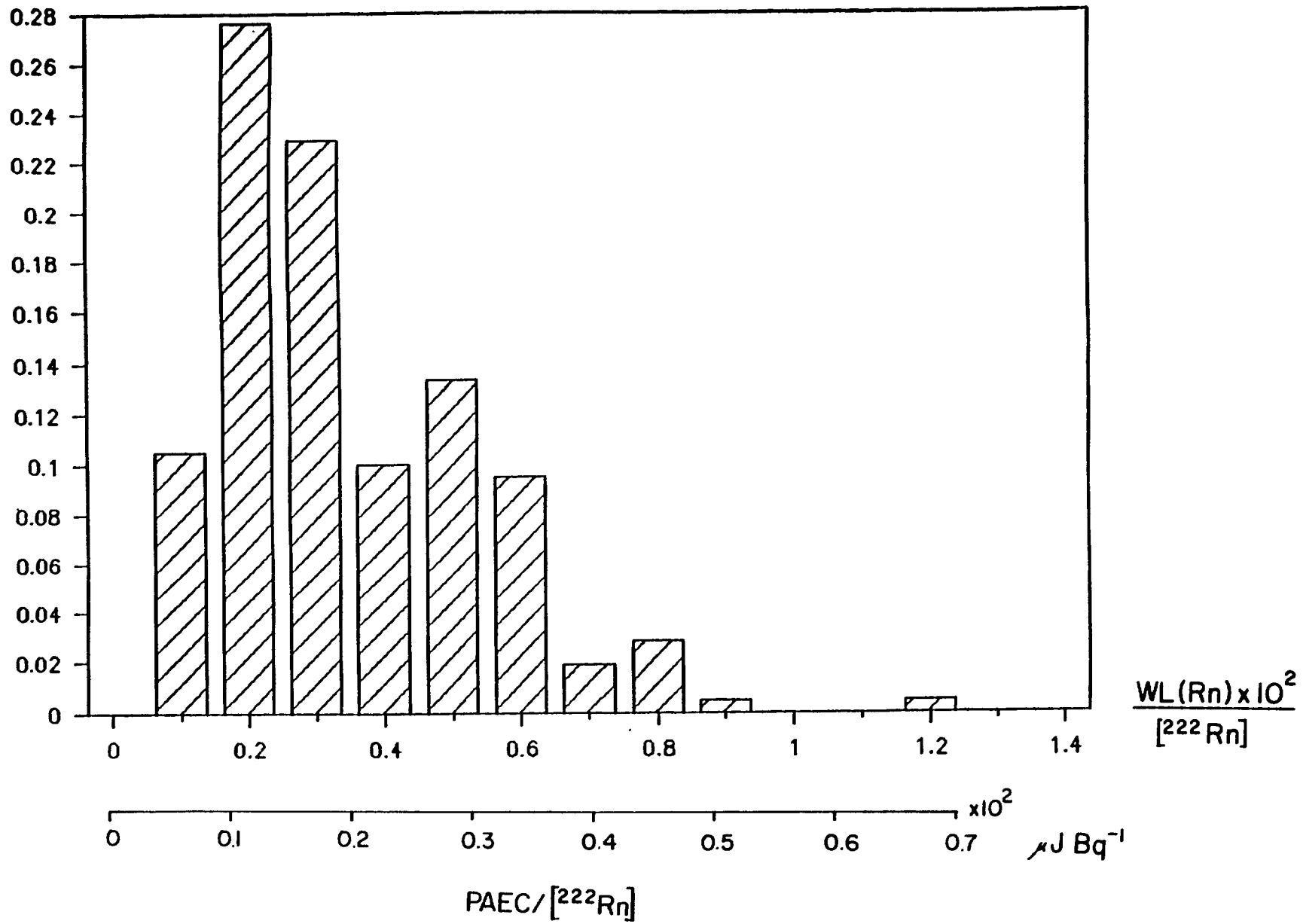
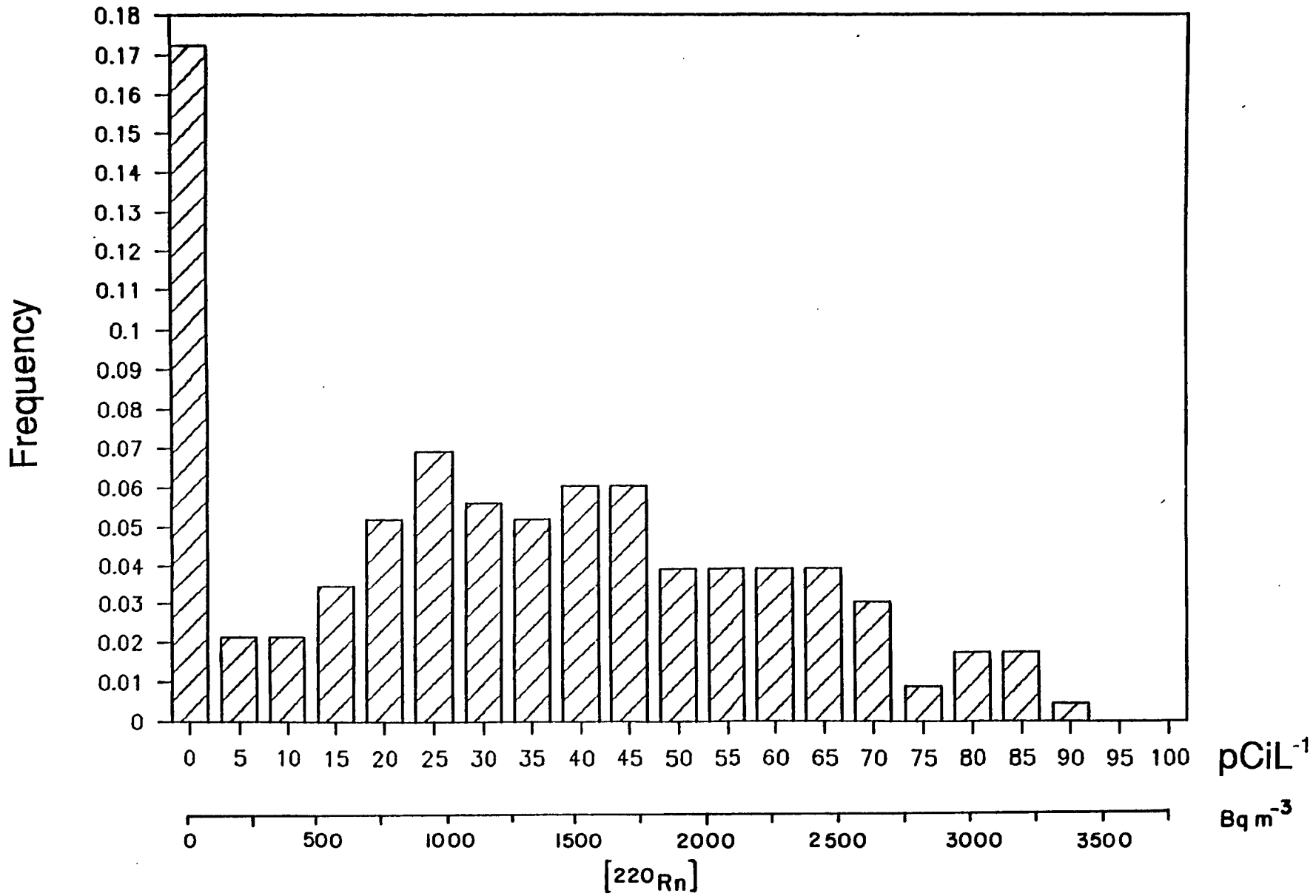


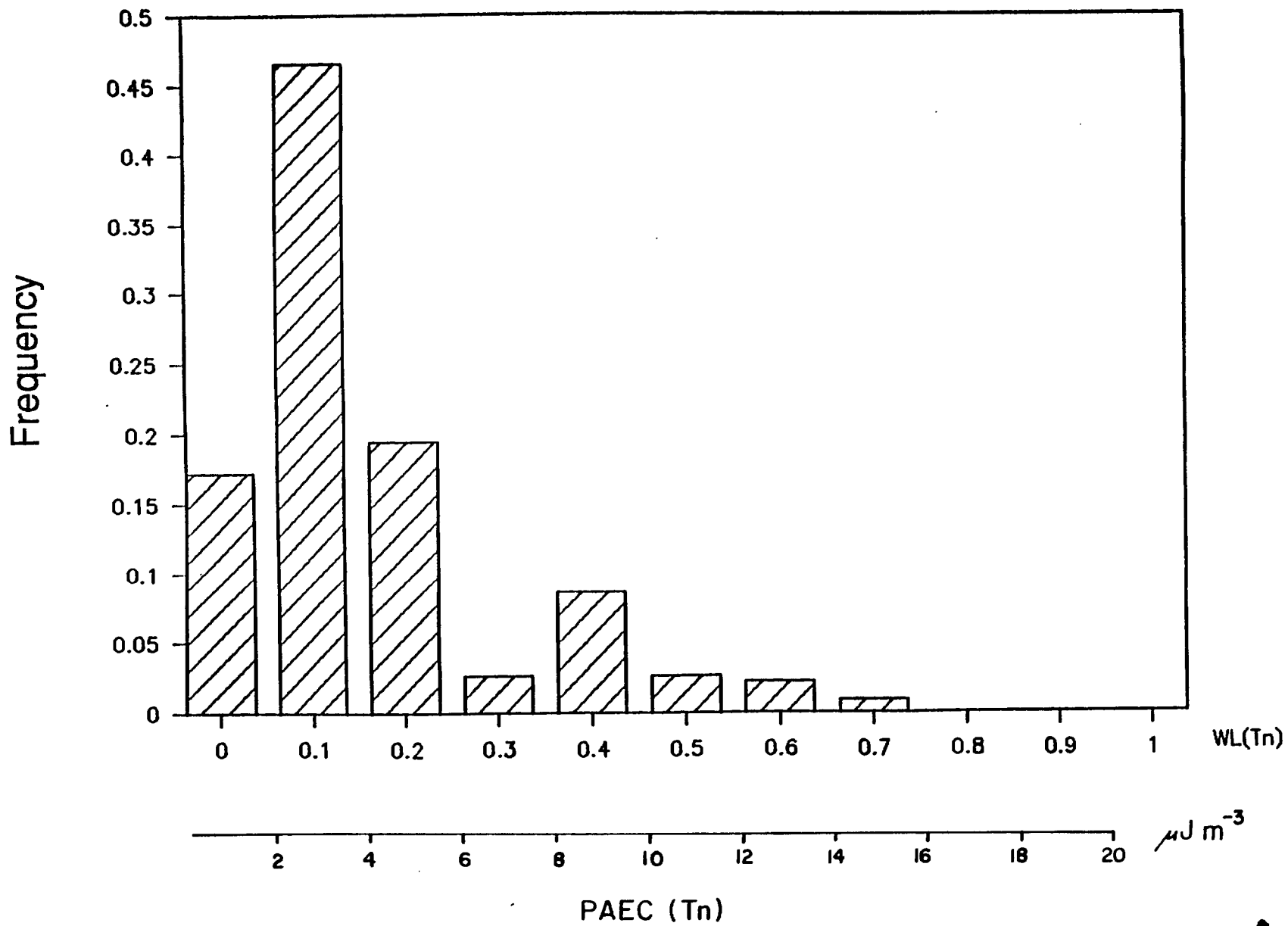
fig. 2



ig. 3



ig. 4



ig. 5

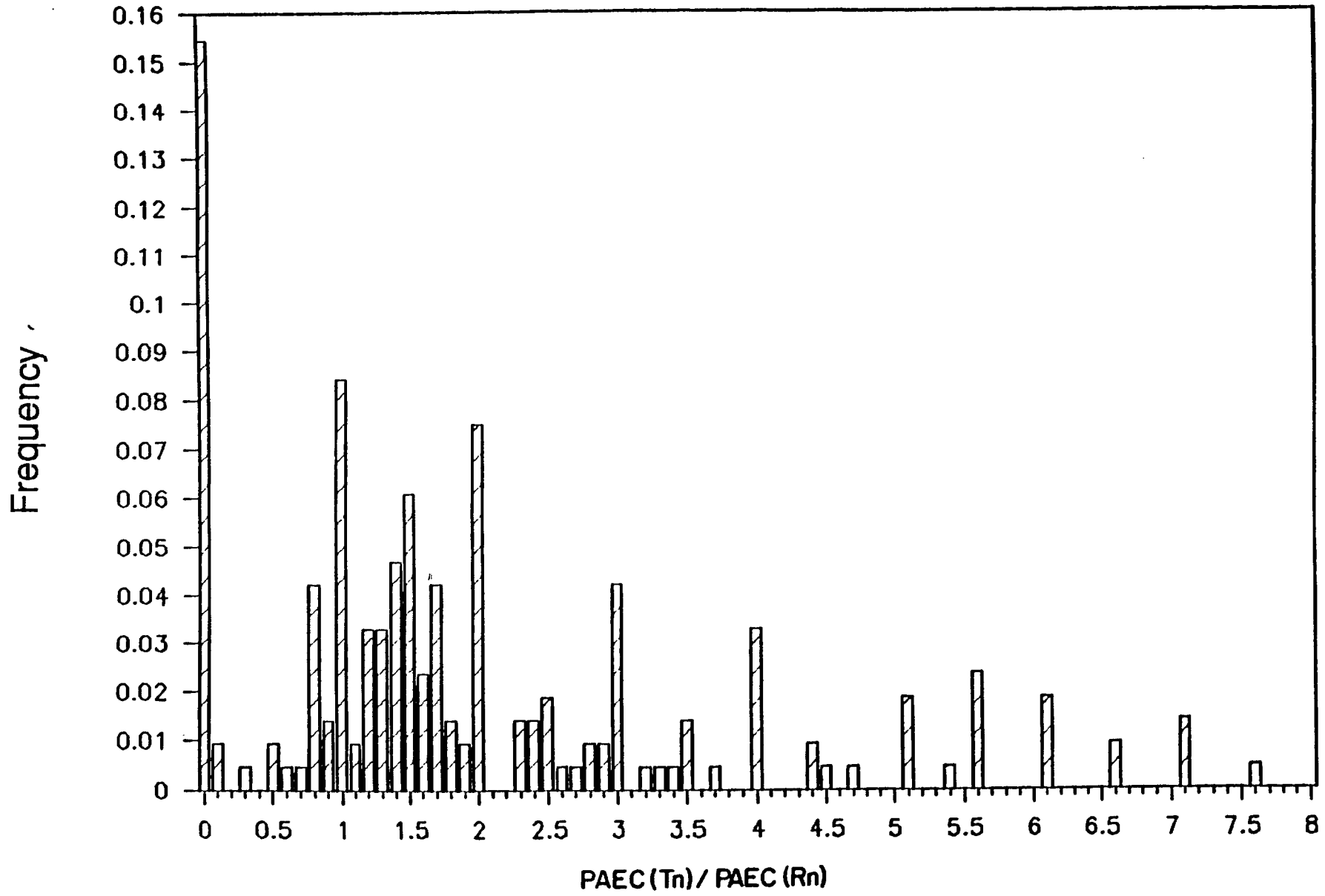
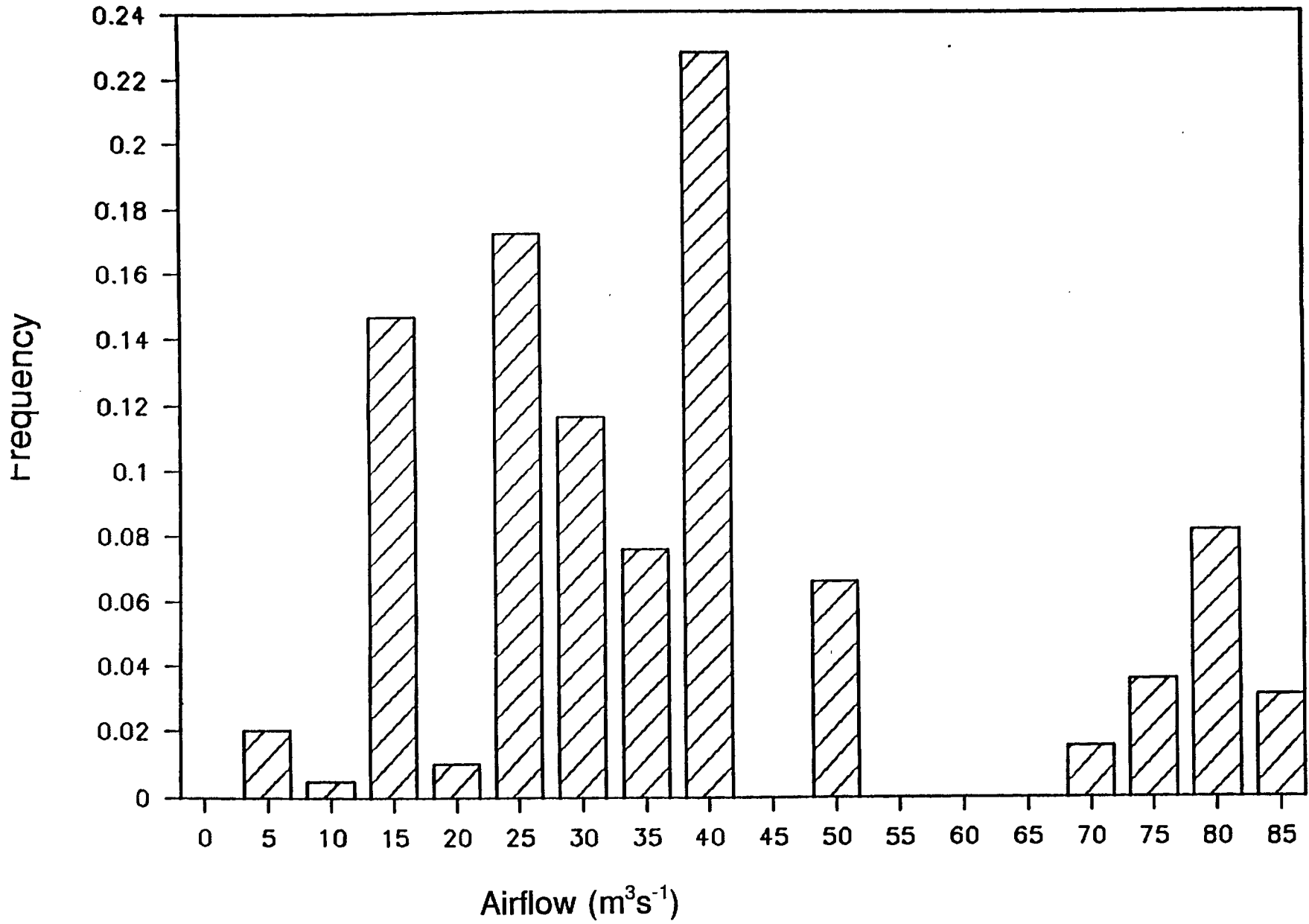
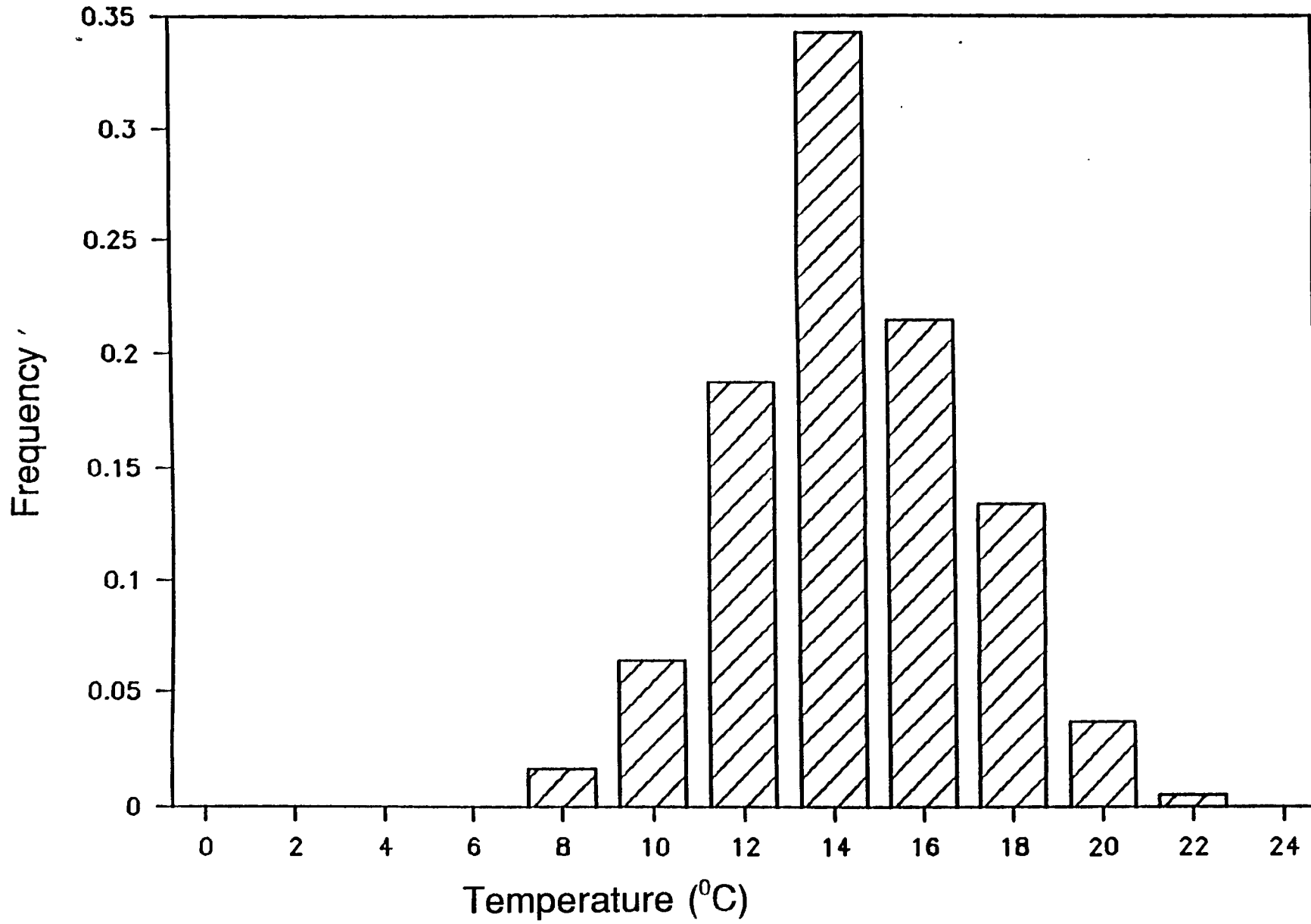


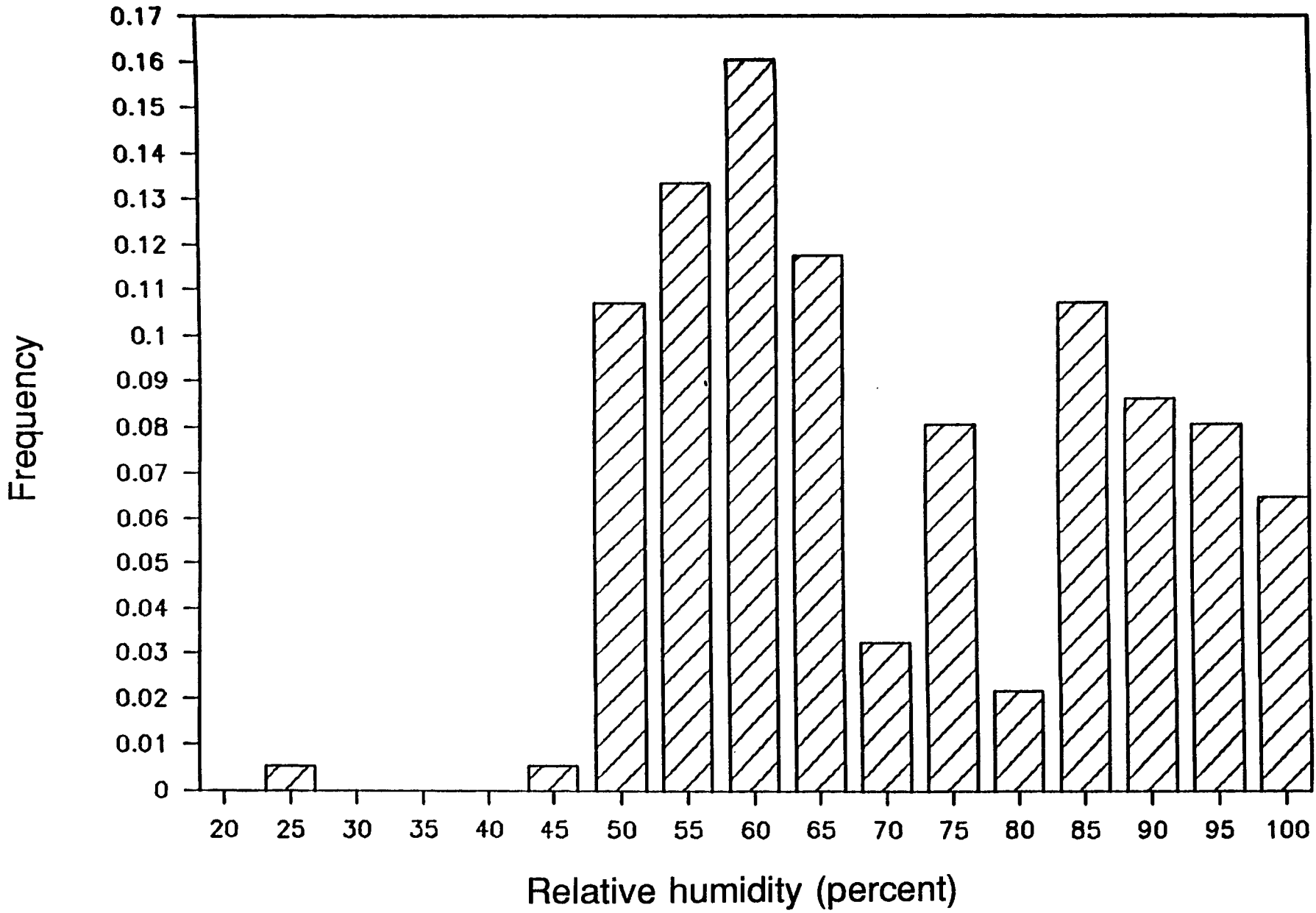
Fig. 6



ig. 7



ig. 8



ig. 9



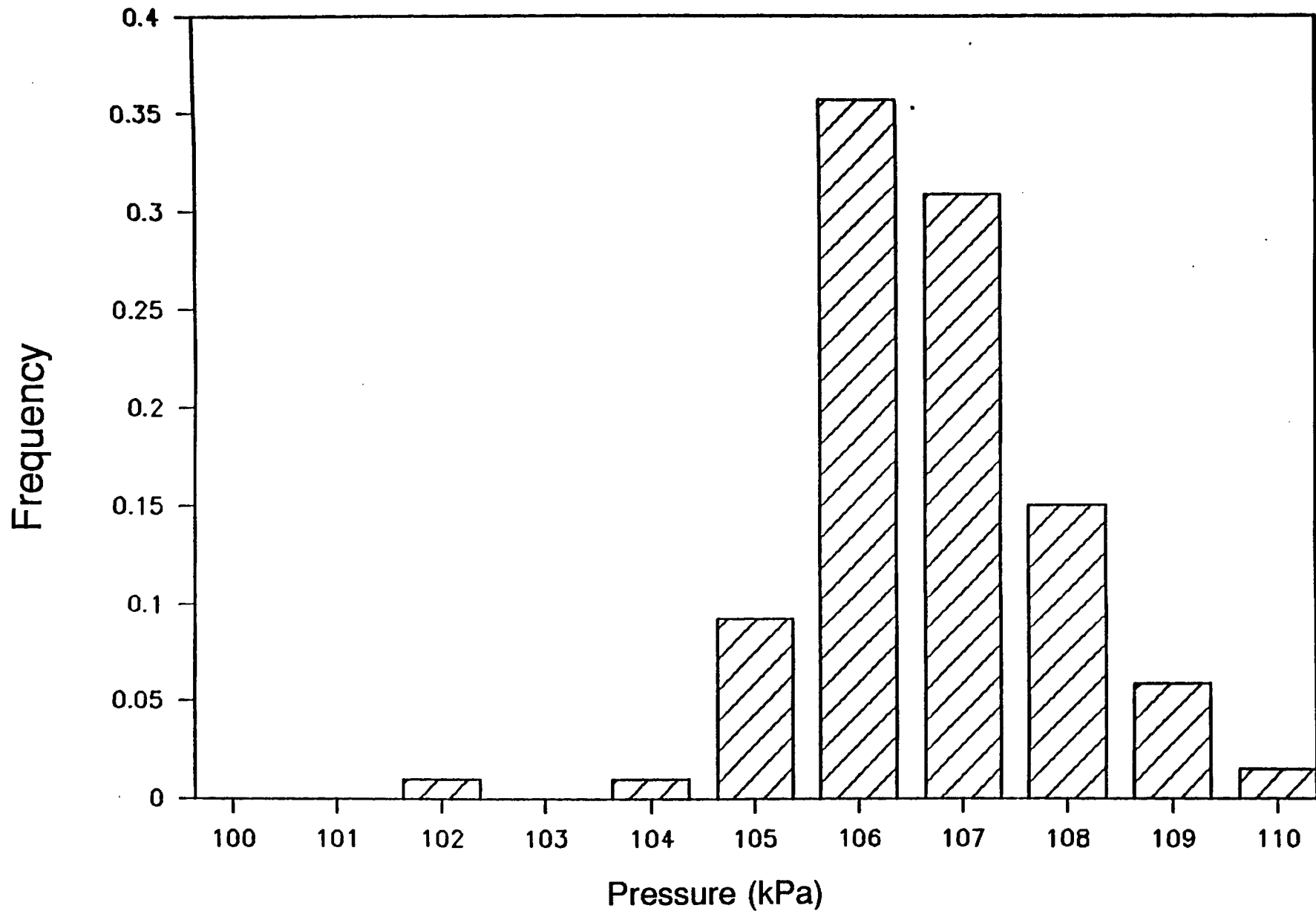


Fig. 10

